

Scalable Multiple Patterning Layout Decomposition Implemented by a Distribution Evolutionary Algorithm *

Yu Chen¹, Yongjian Xu¹, Ning Xu^{1,*}

Abstract

As the feature size of semiconductor technology shrinks to 10 nm and beyond, the multiple patterning lithography (MPL) attracts more attention from the industry. In this paper, we model the layout decomposition of MPL as a generalized graph coloring problem, which is addressed by a distribution evolutionary algorithm based on a population of probabilistic model (DEA-PPM). DEA-PPM can strike a balance between decomposition results and running time, being scalable for varied settings of mask number and lithography resolution. Due to its robustness of decomposition results, this could be an alternative technique for multiple patterning layout decomposition in next-generation technology nodes.

Keywords: multiple patterning lithography, layout decomposition, distribution evolutionary algorithm

1. Introduction

Multiple patterning lithography (MPL) improves the resolution limit of existing lithography technologies, which could then meet the challenge of further decrease of feature size for the next-generation technology nodes [1]. Given a layout specified by features in polygonal shapes, a layout graph (LG) is an undirected graph whose nodes are the given layout's features and where an edge exists if and only if two polygonal shapes are beyond the lithography resolution limit [2]. Multiple patterning layout decomposition (MPLD) partitions a layout into several sections (masks), which is then modelled as a graph coloring problem (GCP).

The GCP can be generally formulated as an integer optimization problem, and a variety of integer linear programming (ILP) methods have been developed to address the MPLD problem [3, 4, 5, 6]. Since the GCP is NP-complete, the ILP methods cannot decompose large-scale layouts efficiently, and it was relaxed to a semidefinite programming (SDP) [7] problem or a linear programming (LP) problem [8]. Although the SDP and LP methods leads to scalability of MPLD to large-scale cases, additional repair processes are needed to get the feasible solutions of GCP, and the relaxation would mathematically lead to solutions different from those of the original MPLD problem. Accordingly, the MPLD problem was also addressed by heuristics [9, 10, 11, 12, 13], and some layout decomposition works based on hybrid lithography have been investigated [14, 15].

According to the number of colors (masks), MPLD problems can be categorized as the double patterning layout decomposition (DPLD) problem [16, 17, 18, 19, 20], the triple patterning layout decomposition (TPLD) problem [21, 22, 23, 24, 25, 26, 27] and the quadruple patterning layout decomposition (QPLD) problem [28], etc. Because the uncolorable modules for varied settings of color number contain different connection topologies, most of the algorithms for MPLD problems are not scalable for varied settings of color number. Yu and Pan [28] proposed an SDP model for QPLD, where extra color assignment strategies are introduced, and the proposed algorithm could be applicable to a k patterning layout decomposition problem with $k \geq 4$. Lin *et al.* [29] proposed a new and effective algorithm for TPLD and QPLD. By utilizing the features in the

*This work was supported in part by the National Key R& D Program of China (2021ZD0114600).

*Corresponding author.

Email addresses: ychen@whut.edu.cn (Yu Chen), xyjcbh188888@163.com (Yongjian Xu), Xuning@whut.edu.cn (Ning Xu)

polyhedron space of the feasible set, the ILP formulation is approximated by the LP relaxation. Jiang and Chang [30] modelled the MPLD problem as an exact cover problem to construct a fast and exact MPLD framework based on augmented dancing links, which can consider the basic and complex coloring rules simultaneously, can maintain density balancing, and can handle quadruple patterning and beyond.

Recently, Li *et al.* [31, 32] proposed an open source layout decomposer named as the *OpenMPL*, where a general framework of MPLD is developed for varied settings of mask number and several alternative optimization schemes including the ILP and the SDP. Although *OpenMPL* incorporates several simplification strategies of the layout graph, the ILP algorithm still suffers from high computational complexity and the solution of SDP is of low quality as usual. In order to develop a scalable MPLD framework that strikes a good balance between the running time and the solution quality, we propose to address it via a distribution evolutionary algorithm based on a population of probability distribution (DEA-PPM) [33], which is based on a novel probability model updated by an orthogonal transformation and a gradual renewal strategy of the distribution model. Meanwhile, the solution space is exploited by deploying a related solution population refined by a tabu search (TS). As a result, the DEA-PPM relying on small populations is expected to achieve robust results on varied settings of the MPLD problem.

The remainder of this paper is organized as follows. Section 2 briefly introduces the framework of *OpenMPL*. In Section 3, the details of DEA-PPM are presented, and Section 4 verifies the competitiveness of DEA-PPM by experimental results. Finally, we conclude the work in Section 5.

2. Multiple Patterning Layout Decomposition based on the OpenMPL

2.1. The Multiple Patterning Layout Decomposition Problem

To address the MPLD problem, the layout is represented by a decomposition graph (DG) consisting of a set of nodes V and two sets of edges, CE and SE , which contain the conflicting edges and stitch edges, respectively [34]. Accordingly, the goal of MPLD is to assign nodes of V with k colors, trying to achieve a nice trade-off between the numbers of conflict and stitch, respectively defined by

$$c_{uv} = \begin{cases} 1 & \text{if } (u, v) \in CE, \\ 0 & \text{otherwise,} \end{cases} \quad (1)$$

and

$$s_{uv} = \begin{cases} 1 & \text{if } (u, v) \in SE, \\ 0 & \text{otherwise.} \end{cases} \quad (2)$$

Then, minimization of conflicts and stitches can be formulated as

$$\min f(\mathbf{x}) = \sum_{(u,v) \in CE} c_{uv} + \alpha \times \sum_{(u,v) \in SE} s_{uv}, \quad (3)$$

where α is the weight parameter, set as 0.1 in this paper [32]. For cases $k = 2, 3, 4$, problem (3) corresponds to the DPLD problem, the TPLD problem and the QPLD problem, respectively.

2.2. Framework of the OpenMPL

As presented in *OpenMPL* [31, 32], the work flow of MPLD starts with generation of the decomposition graph G . Then, size of graph G is reduced by the graph simplification operations, and candidate stitches are inserted to get a modified conflicting graph G' . Before addressing the layout decomposition, G' is further simplified to a reduced graph G'' . Establishing an optimization model for G'' , one can employ a selected optimization algorithm to get the colored graph G'' . At last, the decomposition result of layout can be obtained by recovering the coloring result of G'' to that of the original conflicting graph G . Details of the framework of *OpenMPL* are referred to [31, 32].

OpenMPL incorporates an ILP approach, an SDP approach and a flexible exact cover-based approach as three alternative routines of MPLD. To improve the efficiency of layout decomposition, we proposed to address it by a distribution evolutionary algorithm based on a population of probability models (DEA-PPM) [33], and get the work flow of layout decomposition illustrated in Fig. 1.

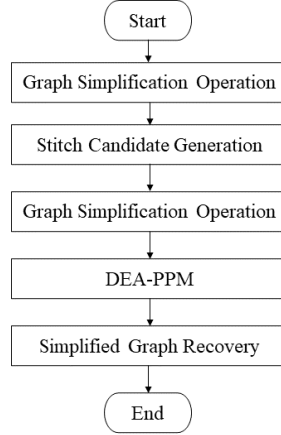


Figure 1: The workflow of layout decomposition based on the *OpenMPL*.

3. A Distribution Evolutionary Algorithm Based on a Population of Probability Model

3.1. The framework of DEA-PPM

Algorithm 1: The framework of DEA-PPM

Input: $G = (V, E)$, color number k
Output: \mathbf{x}_G^*

- 1 initialize $\mathbf{Q}(0)$;
- 2 sample $\mathbf{Q}(0)$ to generate $\mathbf{P}(0)$; /* *uniform initialization* */
- 3 denote the optimal solution in $\mathbf{P}(0)$ as \mathbf{x}_G^* ;
- 4 $\mathbf{p}_1 = \mathbf{x}_G^*$, $\mathbf{p}_2 = \mathbf{x}_G^*$;
- 5 $t \leftarrow 1$;
- 6 **while** *termination-condition 1 is not satisfied* **do**
- 7 $\mathbf{Q}'(t) = \text{OrthExpQ}(\mathbf{Q}(t-1), \mathbf{P}(t-1))$; /* *orthogonal exploration* */
- 8 $\mathbf{P}'(t) = \text{SampleP}(\mathbf{Q}'(t), \mathbf{P}(t-1))$; /* *sampling with inheritance* */
- 9 $(\mathbf{P}(t), \mathbf{p}_1, \mathbf{p}_2, \mathbf{x}_G^*) = \text{RefineP}(\mathbf{P}'(t), \mathbf{p}_1, \mathbf{p}_2, \mathbf{x}_G^*)$;
- 10 /* *refinement of the solution population* */
- 11 $\mathbf{Q}(t) = \text{RefineQ}(\mathbf{P}'(t), \mathbf{P}(t), \mathbf{Q}'(t))$; /* *refinement of the distribution population* */
- 12 $t \leftarrow t + 1$;
- 13 **end**

The framework of DEA-PPM for GCPs is presented in Algorithm 1 [33]. It is implemented based on a distribution population $\mathbf{Q}(t) = (\mathbf{q}^{[1]}(t), \dots, \mathbf{q}^{[np]}(t))$ and a solution population $\mathbf{P}(t) = (\mathbf{x}^{[1]}(t), \dots, \mathbf{x}^{[np]}(t))$, where $\mathbf{x}^{[i]}(t)$ corresponds to $\mathbf{q}^{[i]}(t)$ one by one for all $i \in \{1, \dots, np\}$. For k -coloring of a decomposition graph G , DEA-PPM first initializes the distribution population $\mathbf{Q}(0)$ and the solution population $\mathbf{P}(0)$, and color G by the iterative loop illustrated by Lines 6-12 of Algorithm 1.

The iterative loop attempts to obtain the optimal k -coloring assignment of G by simultaneously evolving the distribution population $\mathbf{Q}(t)$ and the solution population $\mathbf{P}(t)$. In order to obtain the enhanced global exploration, it first performs orthogonal exploration on $\mathbf{Q}(t)$ to obtain $\mathbf{Q}'(t)$. Then, it generates an intermediate solution population $\mathbf{P}'(t)$ and performs a refinement process on $\mathbf{P}'(t)$ to obtain $\mathbf{P}(t+1)$.

Additionally, $\mathbf{Q}'(t)$ is refined to obtain $\mathbf{Q}(t+1)$, and the contents of the loop body are repeatedly executed, updating \mathbf{x}_G^* until termination condition 1 is met. While numbers of conflicts and stitches are

optimized to zero or the maximum number of iterations is reached, the iteration process is ceased and it outputs the corresponding k -coloring assignment of G . Details of the DEA-PPM is referred to Ref. [33].

3.2. Refinement of the solution population

Because the MPLD problem minimizes the number of stitches as well as that of the conflicts, model (3) of MPLD is slightly different with that of the GCP. Accordingly, the refinement process of DEA-PPM, presented in Algorithm 2 is slightly modified to accommodate the MPLD problem well.

Algorithm 2: *RefineP*($\mathbf{P}, \mathbf{p}_1, \mathbf{p}_2, \mathbf{x}_G^*$)

Input: $\mathbf{P}, \mathbf{p}_1, \mathbf{p}_2, \mathbf{x}_G^*$
Output: $\mathbf{P}, \mathbf{p}_1, \mathbf{p}_2, \mathbf{x}_G^*$

```

1  $iter \leftarrow 0, iter\_stag \leftarrow 0;$ 
2  $\mathbf{c}_1 = \mathbf{x}_{G'}^*;$ 
3  $w_2 \leftarrow 0$ 
4 while  $iter\_stag < 6$  do
5    $\mathbf{P}' = MGPX(\mathbf{P}, \mathbf{p}_1, \mathbf{p}_2);$ 
6    $\mathbf{P}' = Tabu(\mathbf{P}');$ 
7   record the best solution in  $\mathbf{P}'$  as  $\mathbf{b};$ 
8   if  $f(\mathbf{b}) < f(\mathbf{p}_1)$  then
9      $w_2 = 1;$ 
10     $iter\_stag = 0;$ 
11     $\mathbf{c}_1 = \mathbf{p}_1, \mathbf{p}_1 = \mathbf{b};$ 
12  else
13     $iter\_stag = iter\_stag + 1;$ 
14  end
15  if  $f(\mathbf{b}) < f(\mathbf{x}_{G'}^*)$  then
16     $\mathbf{x}_{G'}^* = \mathbf{b};$ 
17  end
18  if  $mod(iter, 3) == 0 \&\& w_2 == 1$  then
19     $\mathbf{p}_2 = \mathbf{c}_1;$ 
20     $w_2 = 0;$ 
21  end
22   $\mathbf{P} = \mathbf{P}';$ 
23   $iter = iter + 1;$ 
24 end
25  $\mathbf{P}' = Tabu(\mathbf{P});$ 
26  $\mathbf{p}_1 = \mathbf{b};$ 

```

As presented in Algorithm 2, the iteration budget of *while* loop is set as 6 in this research. Each iteration of the *while* loop starts with a multi-parent greedy partition crossover (MGPX) and a tailored tabu search (TS), and ends with update of the solutions \mathbf{p}_1 , \mathbf{p}_2 and \mathbf{x}_G^* . The MGPX is referred to Ref. [33], and the TS process is presented in Algorithm 3. The TS process for all $\mathbf{x} \in \mathbf{P}$ starts with initialization of the tabu list \mathbf{T} , which is a $k \times n$ matrix where element T_{jv} represents the tabu level of coloring vertex v with color j . Then, an iterative process is performed to improve the quality of \mathbf{x} and to update the tabu list \mathbf{T} .

Improvement of a solution \mathbf{x} is achieved by the *promising* mutations that generate promising solutions. For a vertex v assigned with color i , a random mutation $\langle v, i, j \rangle$ ($j \neq i$) is performed to assign v with color j . While $\langle v, i, j \rangle$ is not forbidden by the tabu list \mathbf{T} , it generates a candidate solution that would replace the coloring scheme \mathbf{x} . To get solutions improved as far as possible, the best promising mutation that contributes to the smallest numbers of conflicts and stitches is employed to generate the promising solution \mathbf{y} , by which the present solution \mathbf{x} is updated if $f(\mathbf{y}) < f(\mathbf{x})$.

Algorithm 3: *Tabu(P)*

Input: \mathbf{P}
Output: \mathbf{P}

```
1 for  $\mathbf{x} \in \mathbf{P}$  do
2    $count \leftarrow 0$ ;
3    $\mathbf{y} = \mathbf{x}$ ;
4   initialize the tabu list  $\mathbf{T}$  to a  $k \times n$  zero matrix;
5   while termination-condition 2 is not satisfied do
6     choose the best legal mutation  $\langle v, i, j \rangle$ ;
7     perform the  $\langle v, i, j \rangle$  in  $\mathbf{y}$ ;
8     Update  $T_{jv}$  of the tabu list  $\mathbf{T}$ ;
9     if  $f(\mathbf{y}) < f(\mathbf{x})$  then
10      |  $\mathbf{x} = \mathbf{y}$ ;
11    end
12     $count = count + 1$ ;
13  end
14 end
```

A random mutation $\langle v, i, j \rangle$ is forbidden by the tabu list if the iteration number $count$ is less than T_{jv} . If a solution \mathbf{y} is generated by implementing $\langle v, i, j \rangle$, the corresponding element of T is updated by

$$T_{j,v} = count + 0.6 * (10 * y_c + y_s) + r,$$

where $count$ is the iteration number of TS, y_c is the number of conflicts in \mathbf{y} , y_s is the number of stitches in \mathbf{y} , and r is an integer randomly sampled in $\{1, \dots, 10\}$.

The iteration of TS is repeated until *termination condition 2* is satisfied, that is, a solution without stitches and conflicts is obtained or the number of iterations reaches the iteration budget $5 * |V|$.

4. Experimental Results

Competitiveness of the proposed MPLD algorithm is validated by result comparison for the ISCAS benchmark problems. The *OpenMPL* decomposer is implemented by C++ on a laptop equipped with Intel Core i7-10750H CPU and a virtual Linux machine. By testing the performance of DEA-PPM on the ISCAS benchmarks, we compare the results by the stitch numbers('st#'), the conflict numbers('cn#'), the cost values('cost') and the CPU running times('time') of ILP, SDP and DEA-PPM. Because DEA-PPM is a stochastic optimization algorithm, the reported results are average values of 10 independent runs, and we also investigate the standard deviations of results to demonstrate its robustness. The scalability of DEA-PPM is validated by varied settings of both the number of masks and the minimum coloring space min_{cs} . To perform a fair comparison, the *OpenMPL* decomposer is run in the single-thread mode. An illustration of the decomposition results is presented for DEA-PPM in Fig. 2.

4.1. Comparison for the TPLD problem with $min_{cs} = 120/100nm$

As presented in [32], *OpenMPL* works well for TPLD of the ISCAS benchmarks, where the minimum coloring spacing min_{cs} is set as $120nm$ for the benchmarks *C432-C7552* and $100nm$ for the benchmarks *S1488-S15850*. Then, we compare the decomposition results of DEA-PPM with those of the ILP and the SDP.

The decomposition results of three algorithms are presented in Tab. 1. For the small value of min_{cs} , vertexes of the decomposition graph would be incident to less edges. The results demonstrate that the proposed DEA-PPM, as a stochastic optimization algorithm, can always achieve the same results as ILP with less running time. Because the SDP method addresses a continuously relaxed problem of model (3),

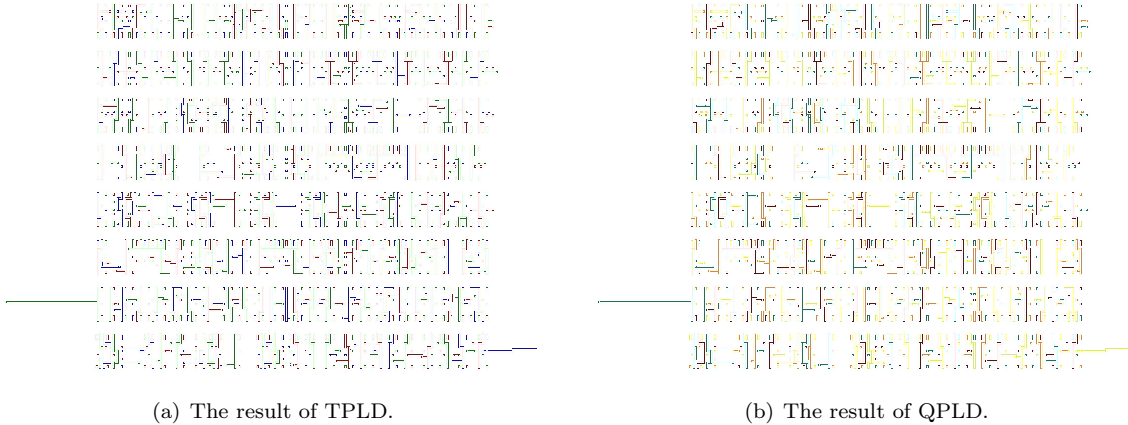


Figure 2: Decomposition results of the layout benchmark $C432$ obtained by the DEA-PPM.

it runs faster than ILP and DEA-PPM, but cannot always converge to the global optimal solutions at all time. Consequently, the decomposition results obtained by the SDP method are generally the same as or worse than those of ILP and DEA-PPM.

It is surprising that the standard deviation of cost is zero, which shows that all independent runs of DEA-PPM converge to the global optimal solution of model (3). Furthermore, the standard deviations of running time are collected in Fig. 3. It is demonstrated that the standard deviation of running time is ignorable for most of the benchmark layouts, except that the standard deviations of running time are about a few seconds for the cases $S35392$, $S38584$ and $S15850$.

Table 1: Result comparison for the TPLD with $min_{cs} = 120/100nm$

Circuit	ILP				SDP				DEA-PPM			
	st#	cn#	cost	time(s)	st#	cn#	cost	time(s)	st#	cn#	cost	time(s)
C432	4	0	0.4	0.38	4	0	0.4	0.09	4	0	0.4	0.30
C499	0	0	0	0.31	0	0	0	0.13	0	0	0	0.25
C880	7	0	0.7	0.52	7	0	0.7	0.14	7	0	0.7	0.46
C1355	3	0	0.3	1.16	3	0	0.3	0.17	3	0	0.3	0.59
C1908	1	0	0.1	0.6	1	0	0.1	0.28	1	0	0.1	0.52
C2670	6	0	0.6	1.29	6	0	0.6	0.51	6	0	0.6	0.60
C3540	8	1	1.8	2.31	8	1	1.8	0.82	8	1	1.8	1.59
C5315	9	0	0.9	2.02	9	0	0.9	1.49	9	0	0.9	1.84
C6288	205	1	21.5	12.57	203	7	27.3	4.32	205	1	21.5	10.48
C7552	23	0	2.3	6.97	23	0	2.3	1.38	23	0	2.3	3.27
S1488	2	0	0.2	0.58	2	0	0.2	0.31	2	0	0.2	0.42
S38417	54	19	24.4	17.62	46	27	31.6	9.31	54	19	24.4	16.13
S35932	40	44	48	43.49	20	64	66	27.5	40	44	48	32.18
S38584	116	36	47.6	41.37	105	48	58.5	28.37	116	36	47.6	35.83
S15850	97	34	43.7	35.53	83	48	56.3	22.62	97	34	43.7	33.68

4.2. Comparison for the TPLD problem with $min_{cs} = 160nm$

To demonstrate the scalability of our proposed method for various lithography technologies, we investigate the TPLD of ISCAS benchmarks by setting the minimum coloring spacing $min_{cs} = 160nm$. Because

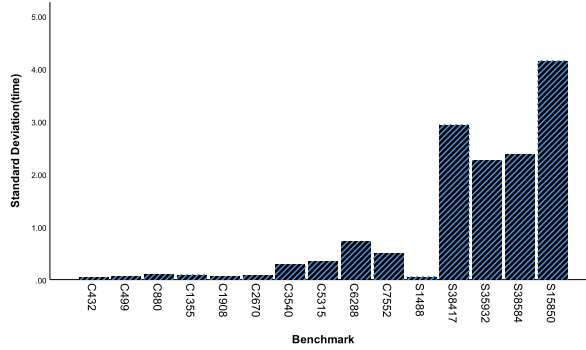


Figure 3: Standard deviations of running time for the TPLD problem with $min_{cs} = 120/100nm$.

the lithography resolution is lower, there could be more conflicting edges in the layout graph, and more stitches would be inserted to get the decomposition graph colorable. Accordingly, the community structure of the decomposition graph could be fuzzier, and decomposition of the layouts is more challenging.

The experimental results collected in Table 2 show that DEA-PPM can deal well with the low-resolution TPLD problem. Compared with the ILP, DEA-PPM contributes to a decrease of more than one order of magnitude of the running time at the expense of a bit increase of the cost values. Meanwhile, the cost values optimized by DEA-PPM are much smaller than the results of SDP, while the running time of DEA-PPM is a bit greater than that of SDP. The histograms illustrated in Fig. 4 show that the standard deviations of cost values are smaller than 3, and those of running time are not more than 10 seconds. Accordingly, DEA-PPM is also robust when applied to address the TPLD problem with $min_{cs} = 160nm$.

Table 2: Result comparison for the TPLD with $min_{cs} = 160nm$

Circuit	ILP				SDP				DEA-PPM			
	st#	cn#	cost	time(s)	st#	cn#	cost	time(s)	st#	cn#	cost	time(s)
C432	17	76	77.7	113.02	19	80	81.9	5.29	17.1	76.9	78.61	6.92
C499	48	278	282.8	339.77	48	279	283.8	10.48	48	278.2	283	16.40
C880	123	103	115.3	244.9	113	115	126.3	9.26	122.4	103.7	115.94	12.06
C1355	116	114	125.6	356.94	109	122	132.9	21.59	118.3	113.9	125.73	17.26
C1908	109	150	160.9	136.82	100	162	172	12.18	106.2	150.7	161.32	16.95
C2670	369	354	390.9	3506.45	358	386	421.8	35.71	369.4	357.2	394.14	41.05
C3540	506	334	384.6	368.65	482	362	410.2	25.08	504	336.4	386.8	40.27
C5315	487	779	827.7	975.58	467	819	865.7	42.6	487	786.2	834.9	71.04
C6288	384	616	654.4	878.71	366	653	689.6	53.76	386.1	622.3	660.91	58.47
C7552	858	843	928.8	3376.73	808	933	1013.8	68.12	851.1	850.6	935.71	89.28

4.3. Comparison for the QPLD problem with $min_{cs} = 200nm$

Besides varied settings of the lithography resolution, we further test the scalability of DEA-PPM by investigating the QPLD problem, where the minimum coloring spacing is set as $200nm$ for 10 ISCAS benchmarks. The test results are listed in Table 3, and Fig. 5 illustrates the standard deviations of both cost values and running time for 10 independent runs. Since the ILP cannot address the *C6288* benchmark in 1 hour, we denote the corresponding results by ‘-’.

The obtained cost values of DEA-PPM are generally better than that of SDP, and its running time is much shorter than that of ILP. It is surprising that compared with the ILP, DEA-PPM achieves better cost values on cases *C432*, *C6288* and *C7552* with much shorter running time. Although the running time of DEA-PPM is a bit longer than that of SDP, the obtained better cost values still demonstrate its

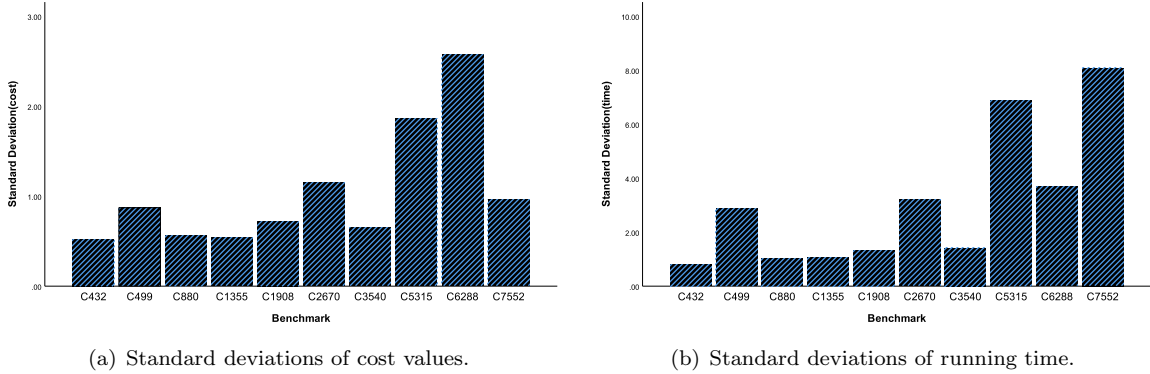


Figure 4: Standard deviations of results obtained by the DEA-PPM for the TPLD problem with $min_{cs} = 160nm$.

competitiveness on the QPLD problem. Fig. 5 demonstrates that the standard deviations of cost value is about 0.5 for all 10 benchmarks, and the running time varies with standard deviations less than 5 seconds for most benchmarks except for *C3540*.

Table 3: Result comparison for the QPLD with $min_{cs} = 200nm$

Circuit	ILP				SDP				DEA-PPM			
	st#	cn#	cost	time(s)	st#	cn#	cost	time(s)	st#	cn#	cost	time(s)
C432	4	14	14.4	61.38	4	12	12.4	1.61	4	13.6	14	1.79
C499	29	7	9.9	123.71	29	8	10.9	8.14	28.9	7.1	9.99	4.72
C880	4	6	6.4	4.1	4	7	7.4	0.58	4	6.5	6.9	1.36
C1355	4	12	12.4	13.44	4	12	12.4	1.41	4	12	12.4	1.65
C1908	10	24	25	50.42	10	24	25	3.94	10	24	25	3.98
C2670	11	24	25.1	225.96	12	25	26.2	5.98	11	24	25.1	4.25
C3540	18	39	40.8	49.94	20	43	45	4.26	18	39	40.8	46.22
C5315	31	38	41.1	90.47	30	40	43	5.63	31	38	41.1	8.77
C6288	-	-	-	-	10	299	300	18.32	8.3	297.9	298.73	31.09
C7552	38	60	63.8	706.97	36	61	64.6	7.66	38	59.1	62.9	11.48

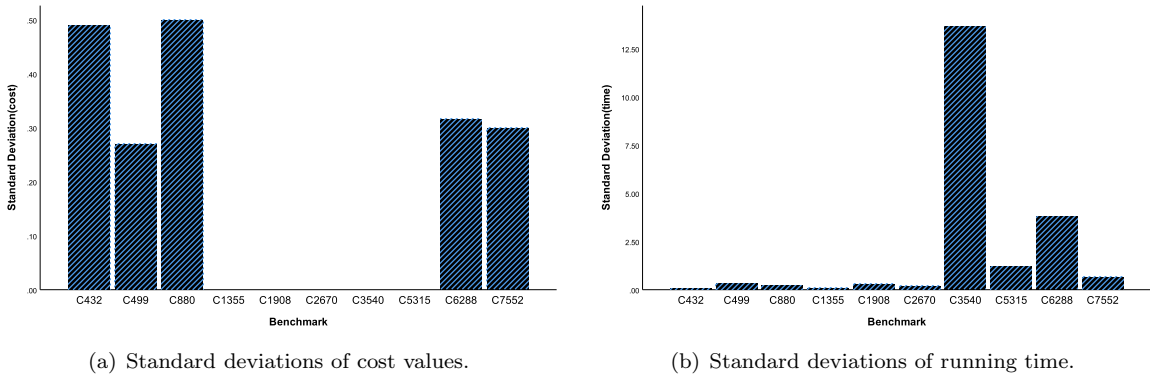


Figure 5: Standard deviations of results obtained by the DEA-PPM for the QPLD problem with $min_{cs} = 200nm$.

5. Conclusion

To develop a scalable layout decomposition scheme adapted for a variety of lithography resolution with different number of masks, we proposed to model the huge-scale decomposition problem as an extended graph coloring problem, which is addressed by a distribution evolutionary algorithm based on a population of probability models (DEA-PPM).

Since the DEA-PPM employs a distribution evolution scheme assisted by the tabu search, it is scalable to varied settings of the MPL layout decomposition problem. Experimental results on ISCAS benchmarks demonstrate that DEA-PPM can strike a good balance between the optimization results and the running time. Despite that DEA-PPM is generally superior to ILP and inferior to SDP in terms of running time, it can obtain for some benchmarks both smaller cost values and less running time, which show that the proposed decomposition method is competitive to the existing decomposition schemes.

Despite the stochastic nature of DEA-PPM, its tailored search strategies leads to small standard deviations of decomposition results, which shows that the proposed method could be an alternative method for the MPLD of layout.

Acknowledgement

We thank Dr. Ning Li for his constructive suggestions to this work.

References

- [1] Y. Ma, X. Zeng, B. Yu, Methodologies for layout decomposition and mask optimization: A systematic review, 2017 IFIP/IEEE International Conference on Very Large Scale Integration (VLSI-SoC) (2017) 1–6.
- [2] A. B. Kahng, C.-H. Park, X. Xu, H. Yao, Layout decomposition for double patterning lithography, in: 2008 IEEE/ACM International Conference on Computer-Aided Design, IEEE, 2008, pp. 465–472.
- [3] B. Yu, K. Yuan, B. Zhang, D. Ding, D. Z. Pan, Layout decomposition for triple patterning lithography, 2011 IEEE/ACM International Conference on Computer-Aided Design (ICCAD) (2011) 1–8.
- [4] B. Yu, S. Roy, J.-R. Gao, D. Z. Pan, Triple patterning lithography layout decomposition using end-cutting, *Journal of Micro/Nanolithography, MEMS, and MOEMS* 14 (2014).
- [5] M. Y. Lin, Y.-L. Li, K.-W. Lin, Color balancing aware double patterning, 2017 International Conference on Applied System Innovation (ICASI) (2017) 284–287.
- [6] X. Li, Z. Zhu, W. xing Zhu, Discrete relaxation method for triple patterning lithography layout decomposition, *IEEE Transactions on Computers* 66 (2017) 285–298.
- [7] B. Yu, Y.-H. Lin, G. Luk-Pat, D. Ding, K. Lucas, D. Z. Pan, A high-performance triple patterning layout decomposer with balanced density, 2013 IEEE/ACM International Conference on Computer-Aided Design (ICCAD) (2013) 163–169.
- [8] Y. Lin, X. Xu, B. Yu, R. Baldick, D. Z. Pan, Triple/quadruple patterning layout decomposition via linear programming and iterative rounding, *Journal of Micro/Nanolithography, MEMS, and MOEMS* 16 (2017).
- [9] S.-Y. Fang, Y.-W. Chang, W.-Y. Chen, A novel layout decomposition algorithm for triple patterning lithography, *DAC Design Automation Conference 2012* (2012) 1181–1186.
- [10] J. Kuang, E. F. Y. Young, An efficient layout decomposition approach for triple patterning lithography, 2013 50th ACM/EDAC/IEEE Design Automation Conference (DAC) (2013) 1–6.
- [11] Y. Zhang, W.-S. Luk, Y. Yang, H. Zhou, C. Yan, D. Z. Pan, X. Zeng, Layout decomposition with pairwise coloring and adaptive multi-start for triple patterning lithography, *ACM Transactions on Design Automation of Electronic Systems (TODAES)* 21 (2015) 1 – 25.
- [12] X. Ke, L. V. Wen, S. Liu, Ant colony algorithm for layout decomposition in double/multiple patterning lithography, 2015 China Semiconductor Technology International Conference (2015) 1–3.
- [13] K.-J. Chen, S.-Y. Fang, Printability enhancement with color balancing for multiple patterning lithography, *IEEE Transactions on Emerging Topics in Computing* 7 (2019) 244–252.
- [14] Y. Yang, W.-S. Luk, H. Zhou, C. Yan, X. Zeng, D. Zhou, Layout decomposition co-optimization for hybrid e-beam and multiple patterning lithography, *IEEE Transactions on Computer-Aided Design of Integrated Circuits and Systems* 35 (2015) 1532–1545.
- [15] X. Li, J. Li, H. Wu, Y.-C. Chen, Discrete relaxation method for hybrid e-beam and triple patterning lithography layout decomposition, *Journal of Ambient Intelligence and Humanized Computing* (2021) 1–11.
- [16] K. Yuan, J.-S. Yang, D. Z. Pan, Double patterning layout decomposition for simultaneous conflict and stitch minimization, *IEEE TRANSACTIONS ON COMPUTER-AIDED DESIGN OF INTEGRATED CIRCUITS AND SYSTEMS* 29 (2) (2010) 185–196. doi:10.1109/TCAD.2009.2035577.

- [17] J.-S. Yang, K. Lu, M. Cho, K. Yuan, D. Z. Pan, A new graph-theoretic, multi-objective layout decomposition framework for double patterning lithography, in: 2010 15TH ASIA AND SOUTH PACIFIC DESIGN AUTOMATION CONFERENCE (ASP-DAC 2010), Asia and South Pacific Design Automation Conference Proceedings, 2010, pp. 623+, 15th Asia and South Pacific Design Automation Conference, Taipei, TAIWAN, JAN 18-21, 2010.
- [18] A. B. Kahng, C.-H. Park, X. Xu, H. Yao, Layout decomposition approaches for double patterning lithography, IEEE TRANSACTIONS ON COMPUTER-AIDED DESIGN OF INTEGRATED CIRCUITS AND SYSTEMS 29 (6) (2010) 939–952. doi:10.1109/TCAD.2010.2048374.
- [19] C.-H. Hsu, Y.-W. Chang, S. R. Nassif, Simultaneous layout migration and decomposition for double patterning technology, IEEE Transactions on Computer-Aided Design of Integrated Circuits and Systems 30 (2) (2011) 284–294. doi:10.1109/TCAD.2010.2079990.
- [20] W. Zhao, H. Yao, Y. Cai, S. Sinha, C. Chiang, Fast and scalable parallel layout decomposition in double patterning lithography, INTEGRATION-THE VLSI JOURNAL 47 (2) (2014) 175–183. doi:10.1016/j.vlsi.2013.09.002.
- [21] B. Yu, G. Garretton, D. Z. Pan, Layout compliance for triple patterning lithography: An iterative approach, in: P. Ackmann, N. Hayashi (Eds.), PHOTOMASK TECHNOLOGY 2014, Vol. 9235 of Proceedings of SPIE, SPIE; BACUS, 2014, conference on Photomask Technology, Monterey, CA, SEP 16-18, 2014. doi:10.1117/12.2066034.
- [22] S.-Y. Fang, Y.-W. Chang, W.-Y. Chen, A novel layout decomposition algorithm for triple patterning lithography, IEEE TRANSACTIONS ON COMPUTER-AIDED DESIGN OF INTEGRATED CIRCUITS AND SYSTEMS 33 (3) (2014) 397–408. doi:10.1109/TCAD.2013.2288678.
- [23] B. Yu, S. Roy, J.-R. Gao, D. Z. Pan, Triple patterning lithography layout decomposition using end-cutting, JOURNAL OF MICRO-NANOLITHOGRAPHY MEMS AND MOEMS 14 (1) (JAN 2015). doi:10.1117/1.JMM.14.1.011002.
- [24] B. Yu, K. Yuan, D. Ding, D. Z. Pan, Layout decomposition for triple patterning lithography, IEEE TRANSACTIONS ON COMPUTER-AIDED DESIGN OF INTEGRATED CIRCUITS AND SYSTEMS 34 (3) (2015) 433–446. doi:10.1109/TCAD.2014.2387840.
- [25] Y. Zhang, W.-S. Luk, Y. Yang, H. Zhou, C. Yan, D. Z. Pan, X. Zeng, Layout decomposition with pairwise coloring and adaptive multi-start for triple patterning lithography, ACM TRANSACTIONS ON DESIGN AUTOMATION OF ELECTRONIC SYSTEMS 21 (1) (NOV 2015). doi:10.1145/2764904.
- [26] X. Ke, H. Jiang, W. Lv, S. Liu, Native conflict aware layout decomposition in triple patterning lithography using bin-based library matching method, in: A. Erdmann, J. Kye (Eds.), OPTICAL MICROLITHOGRAPHY XXIX, Vol. 9780 of Proceedings of SPIE, SPIE; Cymer, 2016, conference on Optical Microlithography XXIX, San Jose, CA, FEB 23-25, 2016. doi:10.1117/12.2219144.
- [27] Y. Kohira, C. Kodama, T. Matsui, A. Takahashi, S. Nojima, S. Tanaka, Yield-aware mask assignment by positive semidefinite relaxation in triple patterning using cut process, JOURNAL OF MICRO-NANOLITHOGRAPHY MEMS AND MOEMS 15 (2) (APR 2016). doi:10.1117/1.JMM.15.2.021207.
- [28] B. Yu, D. Z. Pan, Layout decomposition for quadruple patterning lithography and beyond, 2014 51st ACM/EDAC/IEEE Design Automation Conference (DAC) (2014) 1–6.
- [29] Y. Lin, X. Xu, B. Yu, R. Baldick, D. Z. Pan, Triple/quadruple patterning layout decomposition via linear programming and iterative rounding, JOURNAL OF MICRO-NANOLITHOGRAPHY MEMS AND MOEMS 16 (2) (APR 2017). doi:10.1117/1.JMM.16.2.023507.
- [30] I. Hui-Ru, H.-Y. Chang, Multiple patterning layout decomposition considering complex coloring rules and density balancing, IEEE TRANSACTIONS ON COMPUTER-AIDED DESIGN OF INTEGRATED CIRCUITS AND SYSTEMS 36 (12) (2017) 2080–2092. doi:10.1109/TCAD.2017.2681068.
- [31] W. Li, Y. Ma, Q. Sun, Y. Lin, I. H.-R. Jiang, B. Yu, D. Z. Pan, Openmpl: An open source layout decomposer: Invited paper, 2019 IEEE 13th International Conference on ASIC (ASICON) (2019) 1–4.
- [32] W. Li, Y. Ma, Q. Sun, L. Zhang, Y. Lin, I. H.-R. Jiang, B. Yu, D. Z. Pan, Openmpl: An open-source layout decomposer, IEEE Transactions on Computer-Aided Design of Integrated Circuits and Systems 40 (11) (2021) 2331–2344. doi:10.1109/TCAD.2020.3042175.
- [33] Y. Xu, H. Cheng, Y. Chen, C. Xie, A distribution evolutionary algorithm for graph coloring, arXiv preprint arXiv:2203.15162 (2022).
- [34] K. Yuan, D. Z. Pan, Wisdom: Wire spreading enhanced decomposition of masks in double patterning lithography, in: 2010 IEEE/ACM International Conference on Computer-Aided Design (ICCAD), IEEE, 2010, pp. 32–38.